LETTER

Neutron stars with variable internal heaters

A Letters Journal Exploring the Frontiers of Physics

January 2017

EPL, **117** (2017) 29001 www.epljournal.org
doi: 10.1209/0295-5075/117/29001

Neutron stars with variable internal heaters

E. A. Chaikin[1,2], A. A. Kaurov[3], A. D. Kaminker[1] and D. G. Yakovlev[1]

[1] *Ioffe Institute - Politechnicheskaya 26, 194021, St. Petersburg, Russia*
[2] *Peter the Great St. Petersburg Polytechnic University - Politechnicheskaya 29, 194021, St. Petersburg, Russia*
[3] *Department of Astronomy and Astrophysics, University of Chicago - Chicago, IL 60637, USA*

received 10 October 2016; accepted in final form 21 February 2017
published online 9 March 2017

PACS 97.60.Jd – Neutron stars
PACS 65.90.+i – Other topics in thermal properties of condensed matter
PACS 44.40.+a – Thermal radiation

Abstract – We study thermal radiation of a warm neutron star with a variable shell-like heater located in its crust. The heater and the star are taken to be initially in a stationary state. Then the heat power is increased or decreased for some period of time producing a peak or a dip of the thermal surface emission; afterwards the stationary state is restored. Only a small fraction of the generated heat is thermally emitted through the surface. Time variation of the surface luminosity is weakened and distorted with respect to the variation of the generated heat power; the former variation can be observable only under special conditions —neutron stars are "hiding" their internal temperature variations. These results can be useful for the interpretation of the observations of neutron stars with variable thermal surface emission, particularly, magnetars and transiently accreting neutron stars in low-mass X-ray binaries.

Introduction. – The internal structure of neutron stars (most compact stars containing superdense matter with poorly known properties) is a long-standing fundamental astrophysical and physical problem [1,2]. There is a solid observational evidence that some neutron stars possess internal heat sources of different nature [3–6]. Such internal heaters can affect the evolution of neutron stars which can be of primary importance.

Here we investigate such sources located in a neutron star crust, which is a thin layer under the surface (about 1% of star's mass); it surrounds a superdense, massive and bulky stellar core [1]. To be general, we do not specify the nature of the heater in simulations (but discuss it briefly in the "Conclusions" section). Using a neutron star cooling code, we calculate possible signatures of the heater in the surface emission and analyze the conditions at which these signatures can be observed.

Previously, we have investigated (quasi-)stationary heaters [7,8] and have shown that the strongest effects on the thermal surface emission are produced by the heaters located in the outer crust, not far from the surface. Otherwise the generated heat is mainly conducted to the core and radiated away by neutrinos.

Here we study a variable heater which increases or decreases its power for some time Δt and produces a peak or a dip in the thermal surface emission. Are these variations observable? A similar problem has been studied for short (a few hours) and strong heater's energy generations [9]. We extend these studies for longer Δt (see below) and present the first results.

Simulations. – For simulations, we have used our new one-dimensional cooling code which calculates the evolution of the temperature in a spherically symmetric star with a nucleon core. The code is written in Python programming language. It adopts a one-dimensional mesh with 350 radial spherical cells, from the star's center to the density $\rho_{\rm b} = 10^9\,{\rm g\,cm^{-3}}$. The code is based on the implicit Euler backward method which makes simulations stable under a vast range of initial conditions. It solves for the temperature distribution $T(\rho, t)$ within the star at densities $\rho > \rho_{\rm b}$, taking into account thermal conduction, neutrino cooling and an assumed heating. General relativity effects are included exactly. Microphysics input is mainly the same as in our standard one-dimensional cooling code [10]. In particular, the effects of neutron and proton superfluidities on the neutrino emissivity and heat capacity of the matter are included in the same manner. However, for simplicity, we will neglect these effects here because our heater is sufficiently close to the surface where the effects of superfluidity on heat transport are not important.

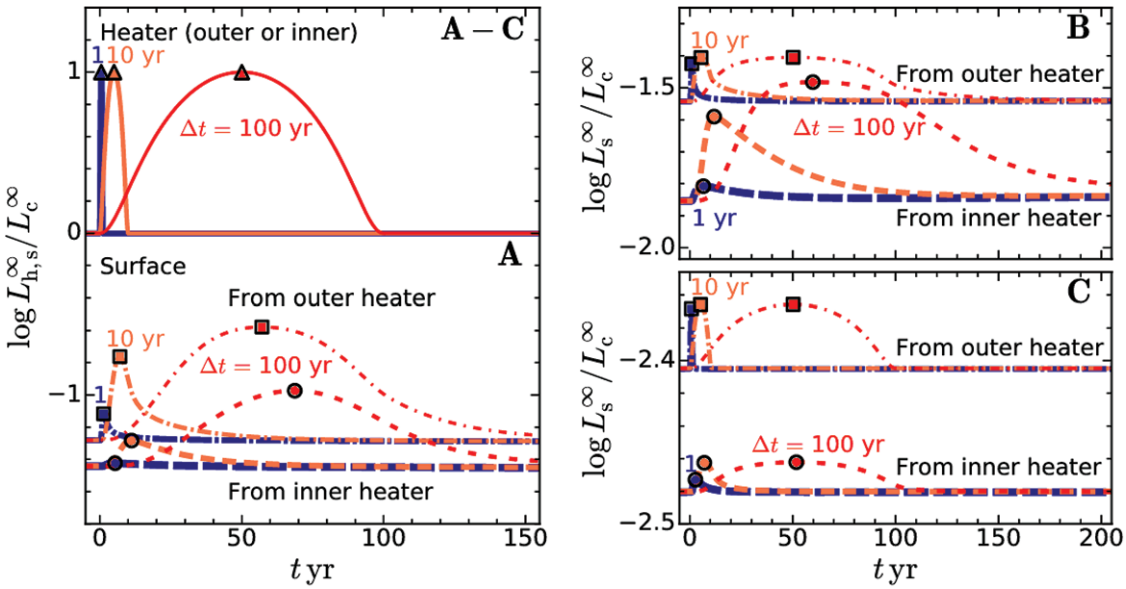

Fig. 1: (Colour online) The peaks of the heater's power $L_{\rm h}^{\infty}(t)$ and the surface thermal luminosities $L_{\rm s}^{\infty}(t)$ *vs.* t for three steady heater powers $L_{\rm c}^{\infty}$ (A, B and C), two heater positions (outer and inner) and three heat variation durations (Δt = 1, 10 and 100 yr), as described in the text. Triangles, squares and circles indicate maxima of $L_{\rm h}^{\infty}(t)$ and $L_{\rm s}^{\infty}(t)$ for the outer and inner heaters, respectively. The energy generation amplitudes are taken to be $H_0 = 9\,H_{\rm c}$.

The effective surface temperature of the star $T_{\rm s}$ is connected to the temperature $T_{\rm b}$ at $\rho = \rho_{\rm b}$ through a special $T_{\rm s} - T_{\rm b}$ relation which is calculated separately using a quasi-stationary plane-parallel approximation [11]. We have employed a recently computed relation [12] for the surface layers made of iron. For surface temperatures $T_{\rm s} \gtrsim 1$ MK of our interest, a typical heat propagation time from $\rho_{\rm b} = 10^9\,{\rm g\,cm^{-3}}$ through this heat blanketing envelope is $t_{\rm th} \sim 1$ d. Therefore, our code allows us to study surface temperature variations not shorter than about 1 d. If we took a standard model of the heat-blanketing envelope with $\rho_{\rm b} = 10^{10}\,{\rm g\,cm^{-3}}$, the "time resolution" of our code would be $t_{\rm th} \sim 1$ yr.

For simulations, we have chosen one neutron star model, with the BSk21 equation of state [13] of nucleon matter in the core. The gravitational mass of the chosen model is $M = 1.4\,M_{\odot}$ and the circumferential radius $R = 12.6$ km. We have approximated the heater by a thin spherical layer ($\rho_1 \le \rho \le \rho_2$). The heat power $Q(\rho, t)$ (erg cm^{-3}s^{-1}) has been taken zero outside this layer and independent of ρ within it. Within the heater, we have set

$$Q(\rho, t) = H_{\rm c} + H_{\rm var}(t), \qquad (1)$$

where $H_{\rm c}$ is a constant stationary heat power, and $H_{\rm var}(t)$ is a variation given by

$$H_{\rm var}(t) = H_0 \sin^2(\pi t/\Delta t), \quad \text{at} \quad 0 \le t \le \Delta t, \qquad (2)$$

with $H_{\rm var}(t) = 0$ otherwise, H_0 being a variation amplitude and Δt a variation duration. The time-integrated heat production of variable energy per cm^3 in the heater is

$$\Delta E_{\rm var} = \int_0^{\Delta t} H_{\rm var}(t)\,{\rm d}t = \frac{1}{2}\,H_0\,\Delta t. \qquad (3)$$

If $H_0 > 0$ we create a heat peak, otherwise ($H_0 < 0$) a heat dip. The previous consideration of Pons and Rea [9] formally corresponds to an instantaneous (delta-function) energy release, $H_{\rm var}(t) = \Delta E_{\rm var}\,\delta(t)$.

At the first stage, using the cooling code, we evolve the star with a constant heat power $H_{\rm c}$ in the heater. Initially the star cools down but eventually it is stabilized by the constant heating [7]; in this steady state the star is non-isothermal inside, the maximum temperature $T = T_{\rm h}$ is reached in the heater. Then at some moment $t = 0$ we vary the heat power in accordance with (2). In response, the surface emission starts to vary but after the heat variation stops, the star returns to its initial stationary state. We have calculated the total heat generation power $L_{\rm h}^{\infty}(t)$ (erg s^{-1}) and the total surface luminosity $L_{\rm s}^{\infty}(t)$, both redshifted for a distant observer.

We have mainly considered two positions of the heater. In the first case (of the so-called "outer heater") we assume $\rho_1 = 10^{11}\,{\rm g\,cm^{-3}}$ and $\rho_2 = 10^{12}\,{\rm g\,cm^{-3}}$. In the second case (of the "inner heater") we take $\rho_1 = 10^{12}\,{\rm g\,cm^{-3}}$ and $\rho_2 = 1.27 \times 10^{13}\,{\rm g\,cm^{-3}}$; the value of ρ_2 is chosen in such a way to have equal $L_{\rm h}^{\infty}(t)$ at the same $H_{\rm c}$, H_0 and Δt for both heaters. In simulations, we have varied $H_{\rm c}$, H_0 and Δt. For heat peaks, we have taken $H_0 = 9\,H_{\rm c}$ (so that in the peak maximum we have $H_0 + H_{\rm c} = 10 H_{\rm c}$), while for dips $H_0 = -H_{\rm c}$ (so that the heat power drops to $H_0 + H_{\rm c} = 0$ at $t = \frac{1}{2}\,\Delta t$). Therefore, we have considered rather pronounced variations.

Results. – Let us discuss typical results. Figures 1 and 2 compare the generated heat power $L_{\rm h}^{\infty}(t)$ with the thermal surface luminosity $L_{\rm s}^{\infty}(t)$ of the star. Figure 1

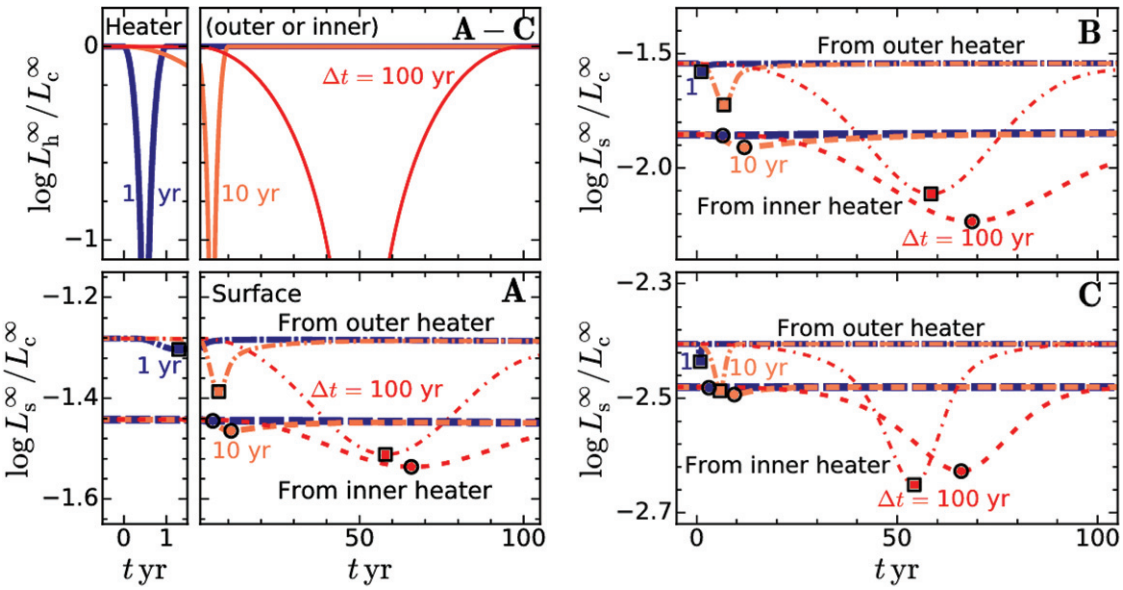

Fig. 2: (Colour online) Same as in fig. 1 but for heat drops down to zero heat intensity at $t = \Delta t/2$; $H_0 = -H_c$. Squares and circles indicate minima of $L_s^\infty(t)$ for the outer and inner heaters, respectively. See text for details.

corresponds to heat peaks, whereas fig. 2 to heat dips. Three cases (A, B and C) in each figure, 1A–C and 2A–C, refer to three stationary heat intensities, $H_c = 5 \times 10^{17}$ (case A), 5×10^{18} (case B) and $5 \times 10^{19}\,\mathrm{erg\,cm^{-3}\,s^{-1}}$ (case C), respectively. The corresponding steady heat powers are $L_c^\infty = 1.7 \times 10^{35}$ (A), 1.7×10^{36} (B) and $1.7 \times 10^{37}\,\mathrm{erg\,s^{-1}}$ (C) (progressively stronger stationary heater and overall warmer star). Note that these ranges of H_c and L_c^∞ are discussed in the literature in the context of magnetic heating of magnetars, *e.g.*, [5,7,8]. Each figure, 1 and 2, shows variations of three durations, $\Delta t = 1$, 10 and 100 yr, produced by the outer and inner heaters.

The three solid curves at the upper left parts A–C of each figure, 1 and 2, show L_h^∞/L_c^∞; these ratios are chosen to be the same for the outer and inner heaters. The solid curves demonstrate variations of $L_h^\infty(t)$.

Any two pairs of three curves on each of the three panels (panels A, B, or C) of fig. 1 or 2 show $L_s^\infty(t)/L_h^\infty$. Each such curve exhibits the surface luminosity $L_s^\infty(t)$ produced either by the outer (thinner and upper dash-dotted lines) or the inner (thicker and lower dashed lines) heater. At the same L_h^∞ and Δt the surface luminosities $L_s^\infty(t)$ depend on the heater's position; the deeper the heater, the lower $L_s^\infty(t)$ (the smaller fraction of heat reaches the surface).

All in all, each figure (1 and 2) shows $L_h^\infty(t)$ and $L_s^\infty(t)$ for three steady heater powers L_c^∞ (A, B and C), two heater positions (inner and outer) and three heat variation durations ($\Delta t = 1, 10$ and 100 yr).

Figure 1 displays the variability of $L_h^\infty(t)$ and $L_s^\infty(t)$ under energy releases at $H_0 = 9\,H_c$. In response to the energy release, the surface emission increases, reaches a maximum and then decreases to its initial pre-burst level. Triangles show the maxima of $L_h^\infty(t)$ (assumed to be at $t = \frac{1}{2}\Delta t$), while squares and circles mark the maxima of $L_s^\infty(t)$ produced by the outer and inner heaters, respectively. In any case only a small fraction of the generated heat is emitted from the stellar surface ($L_s^\infty \ll L_h^\infty$). The behavior of the surface radiation is seen to be drastically dependent of the energy release duration Δt and amplitude H_0, as well as of the pre-burst heater's amplitude H_c, *i.e.*, on the thermal state of the star before the burst. It is convenient to introduce a characteristic heat diffusion time scale $t_{\rm diff}$ from the heater to the surface, the characteristic time scale Δt_s for variability of the surface emission, and the typical heater's temperature $T \approx T_h$. These quantities depend on the heater's parameters. Typically, $t_{\rm diff} \sim$ a few years for the outer heater and it is several times larger for the inner heater; the warmer the star, the larger $t_{\rm diff}$.

Consider, for instance, fig. 1A which is plotted for a relatively low $H_c = 5 \times 10^{17}\,\mathrm{erg\,cm^{-3}\,s^{-1}}$. For the shortest energy release, $\Delta t = 1\,\mathrm{yr}$, the variation of the thermal surface emission is nearly invisible (not detectable). The reason is twofold. First, the total amount of the released energy is not large. Second, the heat propagation time $t_{\rm diff}$ at the decay phase is longer than the energy release duration Δt (so that the surface variability lasts for $\Delta t_s \sim t_{\rm diff} \gg \Delta t$). This disperses $L_s^\infty(t)$ over the long time interval Δt_s, decreasing the peak of the surface emission. The peak shape of $L_s^\infty(t)$ (almost invisible for the scales in fig. 1A) contains a rapid surface luminosity rise ($t_{\rm diff}$ in a pre-burst star) and a slower luminosity decay ($t_{\rm diff}$ in a star heated by the energy release).

For the 10-year-long energy release in fig. 1A, the increase of the surface thermal emission is already quite

visible. The surface luminosity profiles $L_{\rm s}^{\infty}(t)$ have a pronounced peak shape. The peak profiles significantly differ from the profile of the heater's power $L_{\rm h}^{\infty}(t)$ (the upper curve). Specifically, the peaks of $L_{\rm s}^{\infty}(t)$ are smaller, broader, and asymmetrical, whereas the peak of $L_{\rm h}^{\infty}(t)$ is symmetric with respect to $t = \frac{1}{2}\,\Delta t$. In addition, the peaks of $L_{\rm s}^{\infty}(t)$ essentially depend on the heater's position. The peak shifts are naturally explained by a finite diffusion time $t_{\rm diff}$. In our particular case, the peak shift for the outer heater is about 2 years, while the shift for the inner heater is about 7 years.

For the longest energy release displayed in fig. 1A ($\Delta t = 100\,{\rm yr}$) the situation is basically the same but better visible in the figure. The $L_{\rm s}^{\infty}(t)$ peaks are damped, shifted and broadened with respect to the $L_{\rm h}^{\infty}(t)$ peak. The $L_{\rm s}^{\infty}(t)$ peak maximum for the outer heater is only 50% higher than the analogous maximum for the shorter energy release, $\Delta t = 10\,{\rm yr}$, while the $L_{\rm s}^{\infty}(t)$ peak maximum for the inner heater at $\Delta t = 100\,{\rm yr}$ is much higher than the corresponding maximum at $\Delta t = 10\,{\rm yr}$. If $\Delta t = 100\,{\rm yr}$, the characteristic heat diffusion time $t_{\rm diff}$ is shorter than Δt (so that now $\Delta t_{\rm s} \sim \Delta t$). Therefore, very roughly, the situation is quasi-stationary; the heater's power varies slowly and the thermal emission approximately follows these variations. In contrast, the case $\Delta t = 10\,{\rm yr}$ can be treated as intermediate between $\Delta t = 1\,{\rm yr}$ and $\Delta t = 100\,{\rm yr}$ ($t_{\rm diff} \sim \Delta t$). With the growth of Δt the peak shape becomes more symmetric, resembling the shape of $L_{\rm h}^{\infty}(t)$. Now the longer energy release is roughly quasi-stationary, while the shorter one is not.

Even longer energy releases, with $\Delta t \gtrsim 100\,{\rm yr}$, would be more quasi-stationary but hardly detectable (an observer would consider such sources as not variable). Therefore, the most favorable variations to be detected are those from the outer heater of intermediate duration, with Δt from a few to a few tens of years. Another important condition concerns the variation amplitude H_0 of the heat generation. In fig. 1 we have assumed rather strong variations, $H_0 = 9\,H_{\rm c}$. Had we taken lower H_0, the variations of $L_{\rm s}^{\infty}(t)$ would be even weaker.

Figure 1B shows basically the same quantities as fig. 1A but for a 10 times stronger stationary heater ($H_{\rm c} = 5 \times 10^{18}\,{\rm erg\,cm^{-3}\,s^{-1}}$). Then the star is overall warmer. All the effects mentioned above (suppression, shift and broadening of $L_{\rm s}^{\infty}(t)$ peaks with respect to $L_{\rm h}^{\infty}(t)$ ones) are naturally available here but they are quantitatively different. Note a significant dilatation of the $L_{\rm s}^{\infty}(t)$ variation with respect to $L_{\rm h}^{\infty}(t)$, especially for the inner heater; $L_{\rm s}^{\infty}(t)$ varies long after the heater returns to its steady state. Thus, the star will demonstrate a pronounced afterglow.

Finally, fig. 1C shows the same curves as in figs. 1A and B, but for much warmer star, with $H_{\rm c} = 5 \times 10^{19}\,{\rm erg\,cm^{-3}\,s^{-1}}$. As shown in [7–9], this case is special because the temperature in the heater becomes so high ($T_{\rm h} \gtrsim 10^9\,{\rm K}$) that the neutrino cooling in the heater is more efficient than the thermal conduction; the generated heat is mostly carried away by neutrinos. The fraction of heat emitted from the surface becomes very low. When an extra heat is generated, it is taken away by neutrinos. Accordingly, the time variability of the heater in such a warm neutron star will weakly affect the surface emission.

Based on figs. 1A–C we can very roughly distinguish three main regimes of the surface variability of the star.

1) The regime of *dynamic response* to an internal rapid energy release ($\Delta t \lesssim t_{\rm diff}$) in a not too hot star ($T_{\rm h} \lesssim 10^9\,{\rm K}$). It is characterized by a rather rapid rise and longer decay on diffusion time-scales $\Delta t_{\rm s} \sim t_{\rm diff}$. The peak of the surface emission weakly depends on Δt.

2) The regime of *quasi-stationary response* in a not too hot star ($T_{\rm h} \lesssim 10^9\,{\rm K}$) to a slow energy release ($\Delta t \gtrsim t_{\rm diff}$). It produces a peak of the surface emission which resembles the internal energy release, lasts for $\sim \Delta t$, and weakly depends on $t_{\rm diff}$.

3) The regime of *efficient neutrino cooling* of the heater in a hot star ($T_{\rm h} \gtrsim 10^9\,{\rm K}$). It leads to weak variations of the surface emission.

The peak shapes of $L_{\rm s}^{\infty}(t)$ in the dynamical regime qualitatively agree with the shapes obtained previously [9] for very short energy releases. Note that Pons and Rea [9] have used a two-dimensional (2D) cooling code and studied a heater in the form of a hot spot or a spherical layer under the stellar surface. In both cases the authors included the effects of strong magnetic fields, which mainly affect heat conduction, while we have not included such effects here.

Figures 2A–C are essentially the same as 1A–C but they are plotted for heater's drops (to zero intensity, $Q = 0$ at $t = \frac{1}{2}\Delta t$; $H_0 = -H_{\rm c}$) instead of energy outbursts. These drops are naturally accompanied by the dips of the surface emission. Nevertheless, the surface emission drops not to zero but to finite minimum values shown by squares or circles. Such minima are again shifted with respect to the minima of $L_{\rm h}^{\infty}(t)$ due to finite heat diffusion time scales. Other effects of $L_{\rm h}^{\infty}(t)$ dips on $L_{\rm s}^{\infty}(t)$ in fig. 2 are more or less similar to the effects of $L_{\rm h}^{\infty}(t)$ for energy outburts in fig. 1. Were the heater's drops weaker (not to zero intensity), the variations of $L_{\rm s}^{\infty}(t)$ would be even less pronounced.

Figure 3I shows isolines of constant $\log L_{\rm s}^{\infty}$ for a stationary (pre-burst) star supported by a steady heater of fixed amplitude $H_{\rm c}$ (no heater's variations there). The isolines are plotted *vs.* heater's position, $\log \rho_1$ (varied widely over the crust), and amplitude $H_{\rm c}$. For each ρ_1 the inner heater's density ρ_2 is chosen in such a way to give equal $L_{\rm h}^{\infty}$ at a fixed $H_{\rm c}$. The figure summarizes all the information on steady heaters discussed above. In particular, the deeper the heater with fixed $L_{\rm h}^{\infty}$, the smaller $L_{\rm s}^{\infty}$; and at very large $H_{\rm c}$ the surface luminosity saturates (stops to depend on $H_{\rm c}$; see the upper left corner of fig. 3I).

Figures 3II and III illustrate our results on energy releases (fig. 1) and drops (fig. 2). Figure 3II shows the

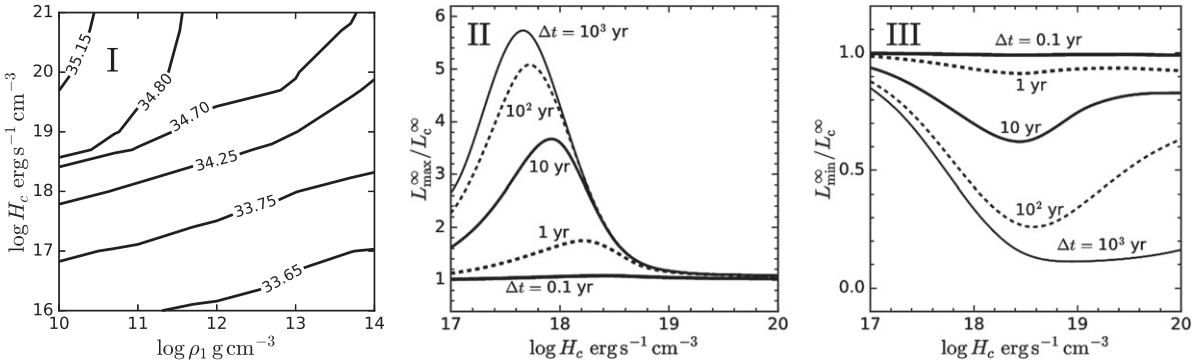

Fig. 3: Panel I: lines of constant $\log L_{\rm s}^\infty$ (erg s^{-1}) (numbers next to the curves) *vs.* ρ_1 and $H_{\rm c}$ for stationary heaters which have the same $L_{\rm h}^\infty$ for any ρ_1 at a fixed $H_{\rm c}$. Other panels: ratios of $L^\infty_{\rm max}/L^\infty_{\rm c}$ (panel II, heat releases, $H_0 = 9\,H_{\rm c}$, as in fig. 1) and ratios of $L^\infty_{\rm min}/L^\infty_{\rm c}$ (panel III, heat dips, $H_0 = -H_{\rm c}$, as in fig. 2) *vs.* $H_{\rm c}$ for the outer heater at five values of $\Delta t = 0.1$, 1, 10, 100 and 1000 yr; $L^\infty_{\rm c}$ is the thermal surface luminosity of the star prior to heater's variations; $L^\infty_{\rm max}$ or $L^\infty_{\rm min}$ are the maximum or minimum surface luminosity for peaks or dips (squares in figs. 1 or 2).

ratios $L^\infty_{\rm max}/L^\infty_{\rm c}$ as a function of $H_{\rm c}$, for the outer heater as an example, at five variability durations $\Delta t = 0.1$, 1, 10, 100 and 1000 yr. Here $L^\infty_{\rm max}$ is the maximum of the surface luminosity (squares in fig. 1) due to the heater's variations. Short variations (*e.g.*, $\Delta t = 0.1$ yr) contain too small energy to affect $L_{\rm s}^\infty(t)$. With increasing Δt at $H_{\rm c} \lesssim 10^{19}$ erg s^{-1} cm^{-3}, the variations of $L_{\rm s}^\infty(t)$ become quite pronounced. The dependence of $L^\infty_{\rm max}/L^\infty_{\rm c}$ on $H_{\rm c}$ at fixed Δt has a peak structure with maximum at $H_{\rm c} \sim 10^{18}$ erg s^{-1} cm^{-3} that is most favorable for heating the surface. Too high $H_{\rm c}$ reduces the variations of $L_{\rm s}^\infty(t)$ because of extra neutrino emission from the heater (see above). Figure 3III shows similar ratios $L^\infty_{\rm min}/L^\infty_{\rm c}$ for heat drops (fig. 2), where $L^\infty_{\rm min}$ is the minimum surface thermal luminosity due to switching the heater off. Again, short variations of Δt do not affect $L_{\rm s}^\infty(t)$, while longer Δt of initially stronger heaters (with larger $H_{\rm c}$) can produce visible drops of $L_{\rm s}^\infty(t)$. Qualitatively, figs. 3II and III indicate that to obtain noticeable variations of the surface emission, one needs an intermediate heater ($H_{\rm c} \sim (1-5)\times 10^{18}$ erg cm^{-3} s^{-1}) and sufficiently long $\Delta t \gtrsim 10$ yr.

Conclusions. – We have simulated thermal evolution of a neutron star with a variable heater placed in a spherical layer in the star's crust. Initially, the heater has been taken static to drive the star to a static state. Then we have increased or decreased the heater's power $L_{\rm h}^\infty(t)$ over some time Δt and returned to the initial steady state afterwards. The problem is if the variations of the thermal surface luminosity $L_{\rm s}^\infty(t)$ are observable.

We have identified three main heat propagation regimes. The first is the dynamical regime in which the variations of $L_{\rm s}^\infty(t)$ are almost independent of Δt, being governed by the thermal diffusion time $t_{\rm diff}$. In the second, quasi-stationary regime the variations of $L_{\rm s}^\infty(t)$ resemble those of $L_{\rm h}^\infty(t)$, being mostly determined by Δt (rather than by $t_{\rm diff}$). The third is the regime of fast neutrino cooling of the heater in a hot star when the $L_{\rm s}^\infty(t)$ variations are strongly damped.

Our main result is that the observability of heater's variations is restrictive —neutron stars are trying to hide their internal activity. To observe its signatures, the heater and its variations have to be strong, but not too strong to avoid efficient neutrino cooling in the heater itself. The heater has to be rather close to the surface (placed at densities $\rho \sim 10^{11}$ g cm^{-3} or lower) to simplify heat transport to the surface. The heater's variation time Δt should be neither short (to produce enough heat) nor very long (to be detectable). Our results agree with the previous consideration [9] but seem more systematic (include studies of dips and of the quasi-stationary regime).

The results have many applications for neutron stars heated from inside, especially from the crust. They may help interpret observations of such stars and clarify the mechanisms for steady-state and variable heating.

Internal heaters can operate in vastly different neutron stars. For instance, they can be young stars (of age $\lesssim 100$ yr) which have not reached the state of internal thermal relaxation (as discussed, *e.g.*, in [8]). They can also be middle-aged isolated neutron stars with many possible reheating mechanisms outlined in [14,15]. Alternatively, they can be old accreting neutron stars which demonstrate bursts or superbursts originated in the outer crust [16–18], and transiently accreting neutron stars in compact low-mass X-ray binaries [3,6] warmed up by deep crustal heating [19–21] and by poorly known shallow heating (*e.g.*, [17]) in accreted matter. The heating of magnetars, associated usually with their strong magnetic fields (*e.g.*, [5] and references therein), seems extremely important for the evolution and bursting activity of magnetars. Moreover, some magnetars are known to be related (*e.g.*, [22]) to high-B pulsars, which possess strong magnetic fields $B \gtrsim 10^{14}$ G but show no magnetar activity (need no internal heaters). However, some magnetars can sometimes transform into high-B pulsars (heater is

switched off) and then back (heater is on). Such processes can be roughly described by our heater outburst or drop models.

The nature of steady and variable heaters in neutron stars (particularly, in magnetars) is far from being clear. The magnetic energy can be mainly stored in the bulk of the star but transported and transformed into heat in the outer layers. Many heating mechanisms in magnetars have been extensively studied (*e.g.*, [4,5,9,23,24] and references therein). They include the evolution of magnetic fields (in the core and the crust) under the effects of rotation, Ohmic decay, Hall drift, ambipolar diffusion (in the core), plastic flows in the crust, mechanical deformations of crustals stresses, the effects of MHD waves and current sheets in the crust, bombardement of stellar surface by particles from magnetosphere, etc. Detailed modeling of these phenomena is complicated; our phenomenological approach can help estimate the efficiency of various heaters.

The ability of neutron stars to greatly damp the effects of variable internal heaters on the surface emission does not mean that such effects are not observable at all. For instance, for very strong outbursts, with $H_0/H_\mathrm{c} \gg 10$, the relative peak of the surface luminosity $L^\infty_\mathrm{max}/L^\infty_\mathrm{c}$ can be observable even for short outbursts, $\Delta t \gtrsim 1\,\mathrm{yr}$, provided the star is not very warm (H_c and L^∞_c are rather small). Our extra calculations show that at each H_0/H_c ratio there exists an optimal pre-burst amplitude H_c which provides maximum $L^\infty_\mathrm{max}/L^\infty_\mathrm{c}$ ratio (*e.g.*, fig. 3II), that depends on Δt. The higher H_0/H_c, the lower the optimal amplitude H_c. For instance, at $H_0/H_\mathrm{c} \sim 3\times10^3$ the optimal amplitude H_c decreases down to 10^{17}–$10^{16}\,\mathrm{erg\ s^{-1}cm^{-3}}$.

Therefore, one can obtain an enhancement of the surface luminosity peak by a factor $\gtrsim$ 10–100 with relaxation tails lasting $\gtrsim 1\,\mathrm{yr}$, typical for the magnetar outbursts [9,25]. In this case the heater should produce a very large amount of energy ($H_0/H_\mathrm{c} \gtrsim 10^3$) at a low pre-burst amplitude H_c. In particular, we confirm the possibility of a strong peak of the surface luminosity $L^\infty_\mathrm{max}/L^\infty_\mathrm{c} \sim 10^2$ with a relaxation tail lasting $\lesssim 10\,\mathrm{yr}$ [26] in accordance with the observations of long outbursts of the central compact X-ray source 1E 161348–5055 in the supernova remnant RCW 103 [27,28].

On the other hand, many magnetar outbursts are sufficiently strong and short. It would be difficult to explain them within the internal heater model unless the heater is placed uncomfortably close to the neutron star surface. This is an indirect argument in favor of the widely discussed hypothesis that the radiation of such outbursts is formed in magnetospheres of magnetars [29].

Our results can be extended to consider a variety of neutron star models (different equations of state and stellar masses, and different models for nucleon superfluidity inside the stars), non-spherical heaters, different models for variability of the heaters; it would also be very important to include the effects of strong magnetic fields and MHD waves. Such extensions are certainly beyond the scope of this work.

* * *

The work by DGY was partly supported by the Russian Foundation for Basic Rresearch, grant 16-29-13009-ofi-m.

REFERENCES

[1] Shapiro S. L. and Teukolsky S. A., *Black Holes, White Dwarfs, and Neutron Stars: The Physics of Compact Objects* (Wiley-Interscience, New York) 1983.

[2] Haensel P., Potekhin A. Y. and Yakovlev D. G., *Neutron Stars. 1. Equation of State and Structure* (Springer, New York) 2007.

[3] Wijnands R., Degenaar N. and Page D., *Mon. Not. R. Astron. Soc.*, **432** (2013) 2366.

[4] Li X., Levin Y. and Beloborodov A. M., *Astrophys. J.*, **833** (2016) 189.

[5] Beloborodov A. M. and Li X., *Astrophys. J.*, **833** (2016) 261.

[6] Cumming A., Brown E. F., Fattoyev F. J., Horowitz C. J., Page D. and Reddy S., ArXiv e-prints, arXiv:1608.07532 (2016).

[7] Kaminker A. D., Potekhin A. Y., Yakovlev D. G. and Chabrier G., *Mon. Not. R. Astron. Soc.*, **395** (2009) 2257.

[8] Kaminker A. D., Kaurov A. A., Potekhin A. Y. and Yakovlev D. G., *Mon. Not. R. Astron. Soc.*, **442** (2014) 3484.

[9] Pons J. A. and Rea N., *Astrophys. J.*, **750** (2012) L6.

[10] Gnedin O. Y., Yakovlev D. G. and Potekhin A. Y., *Mon. Not. R. Astron. Soc.*, **324** (2001) 725.

[11] Potekhin A. Y., Chabrier G. and Yakovlev D. G., *Astron. Astrophys.*, **323** (1997) 415.

[12] Beznogov M. V., Potekhin A. Y. and Yakovlev D. G., *Mon. Not. R. Astron. Soc.*, **459** (2016) 1569.

[13] Potekhin A. Y., Fantina A. F., Chamel N., Pearson J. M. and Goriely S., *Astron. Astrophys.*, **560** (2013) A48.

[14] Yakovlev D. G. and Pethick C. J., *Annu. Rev. Astron. Astrophys.*, **42** (2004) 169.

[15] Page D., Geppert U. and Weber F., *Nucl. Phys. A*, **777** (2006) 497.

[16] in't Zand J. J. M., Cumming A., Triemstra T. L., Mateijsen R. A. D. A. and Bagnoli T., *Astron. Astrophys.*, **562** (2014) A16.

[17] Deibel A., Cumming A., Brown E. F. and Page D., *Astrophys. J.*, **809** (2015) L31.

[18] Deibel A., Meisel Z., Schatz H., Brown E. F. and Cumming A., *Astrophys. J.*, **831** (2016) 13.

[19] Haensel P. and Zdunik J. L., *Astron. Astrophys.*, **227** (1990) 431.

[20] Brown E. F., Bildsten L. and Rutledge R. E., *Astrophys. J.*, **504** (1998) L95.

[21] Haensel P. and Zdunik J. L., *Astron. Astrophys.*, **480** (2008) 459.

[22] Mereghetti S., *Braz. J. Phys.*, **43** (2013) 356.

[23] Viganò D., Rea N., Pons J. A., Perna R., Aguilera D. N. and Miralles J. A., *Mon. Not. R. Astron. Soc.*, **434** (2013) 123.

[24] Li X. and Beloborodov A. M., *Astrophys. J.*, **815** (2015) 25.
[25] Coti Zelati F., Rea N., Papitto A., Viganò D., Pons J. A., Turolla R., Esposito P., Haggard D., Baganoff F. K., Ponti G., Israel G. L., Campana S., Torres D. F., Tiengo A., Mereghetti S., Perna R., Zane S., Mignani R. P., Possenti A. and Stella L., *Mon. Not. R. Astron. Soc.*, **449** (2015) 2685.
[26] Popov S. B., Kaurov A. A. and Kaminker A. D., *Publ. Astron. Soc. Australia*, **32** (2015) e018.
[27] De Luca A., Caraveo P. A., Mereghetti S., Tiengo A. and Bignami G. F., *Science*, **313** (2006) 814.
[28] De Luca A., Mignani R. P., Zaggia S., Beccari G., Mereghetti S., Caraveo P. A. and Bignami G. F., *Astrophys. J.*, **682** (2008) 1185.
[29] Beloborodov A. M., *Astrophys. J.*, **762** (2013) 13.